Published in final edited form as:
J Biomed Opt. 2008 ; 13(3): 030506. doi:10.1117/1.2938700.

Real-time swept source optical coherence tomography imaging of the human airway using a microelectromechanical system endoscope and digital signal processor

Jianping Su[a], **Jun Zhang**[b], **Lingfeng Yu**[b], **Henri G Colt**[c], **Matthew Brenner**[b,c], and **Zhongping Chen**[a,b,*]

[a]University of California, Irvine, Department of Biomedical Engineering, Irvine, California 92612

[b]University of California, Irvine, Beckman Laser Institute, Irvine, California 92612

[c]University of California, Pulmonary and Critical Care Division, Irvine Medical Center, Orange, California 92868

Abstract

A fast-scan-rate swept laser for optical coherence tomography (OCT) is suitable to record and analyze a 3-D image volume. However, the whole OCT system speed is limited by data streaming, processing, and storage. In this case, postprocessing is a common technique. Endoscopic clinical applications prefer onsite diagnosis, which requires a real-time technique. Parallel digital signal processors were applied to stream and process data directly from a data digitizer. A real-time system with 20-kHz axial line speed, which was limited only by our swept laser scan rate, was implemented. To couple with the system speed, an endoscope based on an improved 3-D microelectromechanical motor (diameter 1.5 mm, length 9.4 mm) was developed. *In vivo* 3-D imaging of the human airway was demonstrated.

Keywords

optical coherence tomography; swept laser; microelectromechanical; real time

Optical coherence tomography (OCT) is a noninvasive, noncontact imaging modality that uses coherent gating to obtain high-resolution cross-sectional images of tissue microstructure.[1] The 3-D microstructure image volume reveals more morphological information than 2-D images, which is critical in clinical applications such as early-stage cancer detection.[2-5] Currently, a swept laser source for OCT can attain a scan rate higher than 100 kHz, which is suitable to record and analyze a 3-D image volume.[6-8] To acquire a 3-D image volume, a fast 2-D image frame-rate, which is determined by the swept laser scan rate, the imaging endoscope rotational speed, and the data processing speed, is needed. Our swept laser scan rate was 20 kHz, which was sufficient to realize a video-rate 2-D image. The OCT imaging endoscope rotational speed is determined by the high spinning speed of the microelectromechanical (MEMS) motor. The MEMS motor-based endoscope design has several advantages.[5,9] It decouples the rotational torque transfer from the optical fiber to the image probe, thus eliminating the related polarization effect of the spinning image probe. With the small size of the MEMS motor, the whole endoscope package is small and flexible enough to be suitable for clinical applications.

*Tel: 949–824–4713; E-mail: z2chen@uci.edu

Compared to the previous one, the motor diameter decreased 30%, from 2.2 mm to 1.5 mm; and the length decreased 27%, from 13 mm to 9.4 mm.[5] Currently, the bottleneck of the entire system speed is the data processing speed, which is limited by the CPU's processing power. Postprocessing is commonly used. A real-time technique enables onsite diagnosis and is preferable for endoscopic clinical examinations. Furthermore, a real-time technique has been demonstrated in time-domain OCT. One method is to accelerate signal processing based on hardware, including the digital autocorrelator, the field-programmable gate array (FPGA), and the digital signal processor (DSP).[10,11] An alternative method is to fully utilize the CPU's processing power based on a multithreading software technique.[12] In our study, the DSP board and the coupled digitizer were used for real-time data acquisition and image processing for the high-speed swept-source OCT. The digitizer streamed the data directly to the DSP board by a custom-designed auxiliary bus. The computer bus, which was the potential speed bottleneck for data streaming, was bypassed. Parallel data processing was applied with the DSP board. Specifically, each DSP processed the image frame independently. Although we demonstrated real-time processing with a scan rate of only 20 kHz, an estimated 90-kHz scan rate real-time processing can be achieved by combining a digitizer and a DSP board. A real-time image display of the *in vivo* human airway was achieved with a DSP and a MEMS motor-based endoscope.

Our swept-source OCT system and MEMS motor endoscope are shown in Fig. 1. The swept light source (center wavelength 1310 nm, FWHM bandwidth 100 nm, 20-kHz scan rate; Santec Corporation, Komaki, Aichi, Japan) output was 5 mW. The 1×2 coupler split the output power. We coupled 80% of the output power into the sample arm and the remaining 20% into the reference arm. The reference power was attenuated by an adjustable neutral density attenuator to obtain maximum sensitivity. Two circulators were used in both the reference and sample arms to redirect the back-reflected light to a 2×2 fiber coupler (50/50 split ratio) for balanced detection. The measured axial and lateral resolutions of our OCT system in the air were 8 μm and 20 μm, respectively. The image range depth was 2.9 mm. The measured sensitivity of the OCT system with a MEMS motor endoscope was 107 dB. The 6-dB sensitivity rolloff occured at 2.2 mm. A software dispersion compensation algorithm was applied to cancel the dispersion generated by the endoscope optics.[13]

In the sample arm, the MEMS rotational motor-based endoscope was connected. Figure 1 shows the endoscope. The 1310-nm single-mode optical fiber, the 1.3-mm grin lens, the 1.5-mm MEMS motor, and the reflected mirror were packaged inside the biocompatible fluorinated ethylene-propylene (FEP) tube of the endoscope. The size of the driving coils, a key component of the MEMS motor, was reduced due to the improvement of manufacturing technology. Thus, the whole motor became smaller. The diameter was 1.5 mm and the length was 9.4 mm. A total of four wires was used to connect the motor and outside circuit. Two wires were used to supply the 3 volts of DC voltage. One wire transferred the encoded revolutions per minute (RPM) signal, and one wire controlled the rotational direction. The outside circuit implemented the feedback control by adjusting the supply voltage according to the encoded RPM signal, which increased the stability of the rotational speed. A two-stage, 40:1 ratio micro gear head was placed in front of the rotational shaft to smooth the step motion, which was designed to achieve an optimal rotational speed of 30 frames/second. In the experiment, the motor speed was set to 19.5 frames/second to synchronize with the OCT system speed. The outside linear transversal stage pulled the entire endoscope back at 0.4 mm/sec to realize a 3-D helix scan. A total of 400 image slices were processed and displayed in 20.5 seconds.

In the detection arm, the signal collected by the photodetectors was digitized by a 14-bit data acquisition board (PDA14, Data Acquisition Signal Waveform Digitizer, Signatec Inc., Newport Beach, California) sampling at 25 M samples/second, and the number of data points for each axial line (A-line) data acquisition was 1024. The A-line data acquisition start trigger

for the digitizer was generated by the swept source. The digitizer outputted the A-line data directly to the DSP board (PMP1000, Parallel Digital Signal Processing Board, Signatec Inc., Newport Beach, California) through a custom-designed auxiliary bus. The complex analytical depth encoded signal was converted from the detected fringe signal by calibration, resampling, dispersion compensation, and fast Fourier transform. The structure image was reconstructed from the amplitude term of the complex depth encoded signal. In the DSP board, eight DSPs (C6414T, Texas Instruments Inc.) were programmed to work in parallel to implement the above algorithm. Figure 2(a) shows the data flow in the DSP board. The digitized data were fed sequentially into the DSP board from the digitizer. Each DSP handled a 1024 A-line image frame independently with the help of a scheduler. The resulting structure image was sent to the monitor in the same order as the input. The processing power from the DSPs was able to handle a 20-kHz A-line rate. In a simulation test, a square waveform of 90 kHz was set as the A-line trigger. An arbitrary waveform was acquired by the data acquisition board at 100 M samples/second. The 2048 A-line image frames were processed. The 43.9 frames/second image output rate was monitored. The test result indicated that a 90-kHz scan rate real-time processing could be achieved. Figure 2(b) shows the comparison performance test between the DSP and the Intel Xeon core duo CPU. The estimated performance from the DSP board was 3 times faster than the Dell Precision Workstation 690 with Intel 3-GHz Quad Core CPU in terms of fast Fourier transformation.

The MEMS motor-based endoscope was introduced into the human airway under visual guidance from a rigid bronchoscope. The outer diameter of the endoscope was 2.2 mm. Figure 3 shows the segmental human lower left lobe bronchus. In Fig. 3(a), the layer-like structure from the 11 o'clock to 5 o'clock positions shows the posterior membrane. The motor wire blocked part of the signal and caused the dent artifact. Figure 3(b) shows the 3-D reconstruction image volume, which was rebuilt from 400 slices. The stepping distance between 2-D frames was 20.5 um. Figure 3(c) shows the reconstructed longitudinal image slice between the two arrows in Fig. 3(b). The epithelium, lamina propria, and elastic lamina can be seen.

Figure 4 shows segmental human distal trachea. In Fig. 4(a), the notch between the trachea and the posterior membrane can be seen. Some parts of the trachea were outside the OCT image range. A mask was applied to the image to suppress the FEP tube mirror artifact, which generated a constant radial line at a depth of around 0.5 mm beneath the surface. From the 3-D reconstruction in Fig. 4(b), the notch is clearer. The longitudinal length of the image volume was 8.2 mm. The stepping distance between the 2-D frames was 20.5 um. Figure 4(c) shows the reconstructed longitudinal image slice between the two arrows in Fig. 4(b); the cartilage arc can be seen in the middle.

In conclusion, a real-time swept source OCT system with a 20-kHz A-line speed was demonstrated by using multiple DSPs. An *in vivo* human airway 3-D image volume was acquired by a MEMS motor-based endoscope. The estimated performance from the pair of digitizers and the DSP board could support the swept laser with a 90-kHz scan rate.

Acknowledgments

This work was supported by research grants from the National Institutes of Health (EB-00293, CA-91717, and RR-01192), the Air Force Office of Scientific Research (FA9550-04-1-0101), and the Beckman Laser Institute Endowment.

References

1. Huang D, Swanson EA, Lin CP, Schuman JS, Stinson WG, Chang W, Hee MR, Flotte T, Gregory K, Puliafito CA, Fujimoto JG. Optical coherence tomography. Science 1991;254:1178–1181. [PubMed: 1957169]

2. Wojtkowski M, Srinivasan V, Fujimoto JG, Ko T, Schuman JS, Kowalczyk A, Duker JS. Three-dimensional retinal imaging with high-speed ultrahigh-resolution optical coherence tomography. Ophthalmology 2005;112:1734–1746. [PubMed: 16140383]

3. Yun SH, Tearney GJ, Vakoc BJ, Shishkov M, Oh WY, Desjardins AE, Suter MJ, Chan RC, Evans JA, Jang I-K, Nishioka NS, de Boer JF, Bouma BE. Comprehensive volumetric optical microscopy in vivo. Nat. Med 2006;12:1429–1433. [PubMed: 17115049]

4. Adler DC, Chen Y, Huber R, Schmitt J, Connolly J, Fujimoto JG. Three-dimensional endomicroscopy using optical coherence tomography. Nat. Photonics 2007;1:709–716.

5. Su J, Zhang J, Yu L, Chen Z. *In vivo* three-dimensional microelectromechanical endoscopic swept source optical coherence tomography. Opt. Express 2007;15:10390–10396. [PubMed: 19547391]

6. Oh WY, Yun SH, Tearney GJ, Bouma BE. 115 kHz tuning repetition rate ultrahigh-speed wavelength-swept semiconductor laser. Opt. Lett 2005;30:3159–3161. [PubMed: 16350273]

7. Huber R, Wojtkowski M, Fujimoto JG. Fourier domain mode locking (FDML): A new laser operating regime and applications for optical coherence tomography. Opt. Express 2006;14:3225–3237. [PubMed: 19516464]

8. Huber R, Adler DC, Fujimoto JG. Buffered Fourier domain mode locking: unidirectional swept laser sources for optical coherence tomography imaging at 370,000 lines/ s. Opt. Lett 2006;31:2975–2977. [PubMed: 17001371]

9. Tran PH, Mukai DS, Brenner M, Chen Z. *In vivo* endoscopic optical coherence tomography by use of a rotational microelectromechanical system probe. Opt. Lett 2004;29:1236–1238. [PubMed: 15209258]

10. Westphal V, Yazdanfar S, Rollins AM, Izatt JA. Real-time, high velocity-resolution color Doppler optical coherence tomography. Opt. Lett 2002;27:34–36. [PubMed: 18007707]

11. Yan S, Piao D, Chen Y, Zhu Q. Digital signal processor-based real-time optical Doppler tomography system. J. Biomed. Opt 2004;9:454–463. [PubMed: 15189082]

12. Park, B. Hyle; Pierce, MC.; Cense, B.; de Boer, JF. Real-time multi-functional optical coherence tomography. Opt. Express 2003;11:782–793. [PubMed: 19461791]

13. Cense B, Nassif N, Chen T, Pierce M, Yun S-H, Park B, Bouma B, Tearney G, de Boer J. Ultrahigh-resolution high-speed retinal imaging using spectral-domain optical coherence tomography. Opt. Express 2004;12:2435–2447. [PubMed: 19475080]

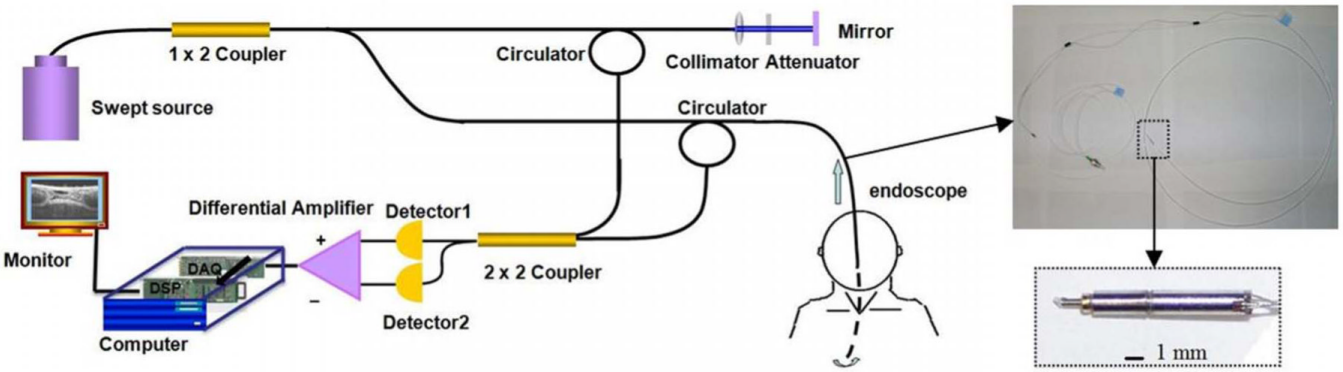

Fig. 1.

(a) Real-time swept-source OCT system setup. A swept laser source with a 20-kHz A-line scan rate was coupled into a fiber-based Michelson interferometer. (b) Endoscope in the sample arm inserted into the patient's airway (top), and the 1.5-mm MEMS motor (bottom). The OCT signal was digitized by the digitizer and sent directly to the DSP board. The output tissue structure image from the DSP board appears in the monitor.

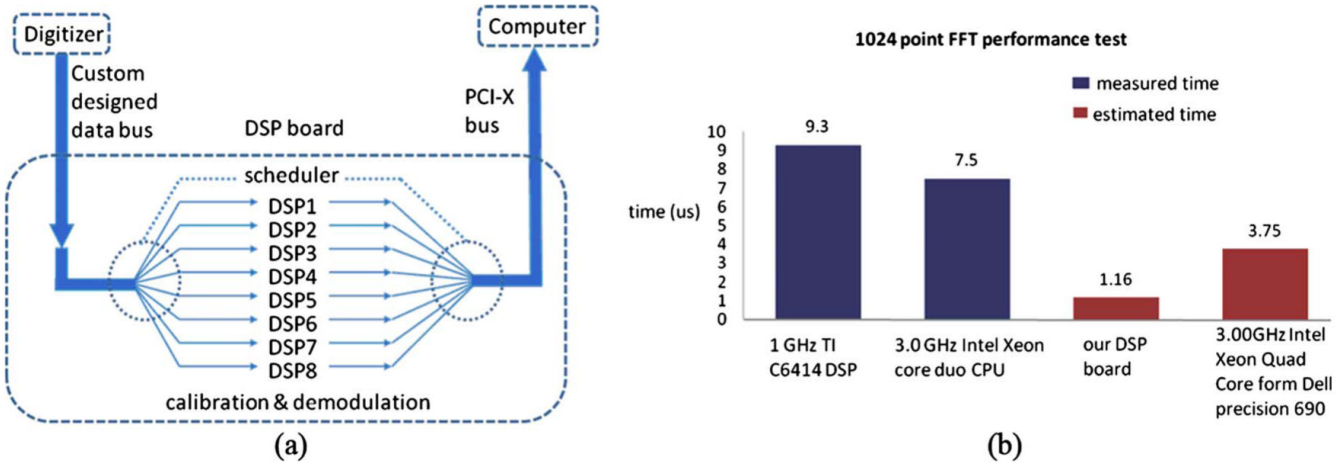

Fig. 2.

(a) Data flow in the DSP board. (b) Performance comparison test between the DSP and the CPU.

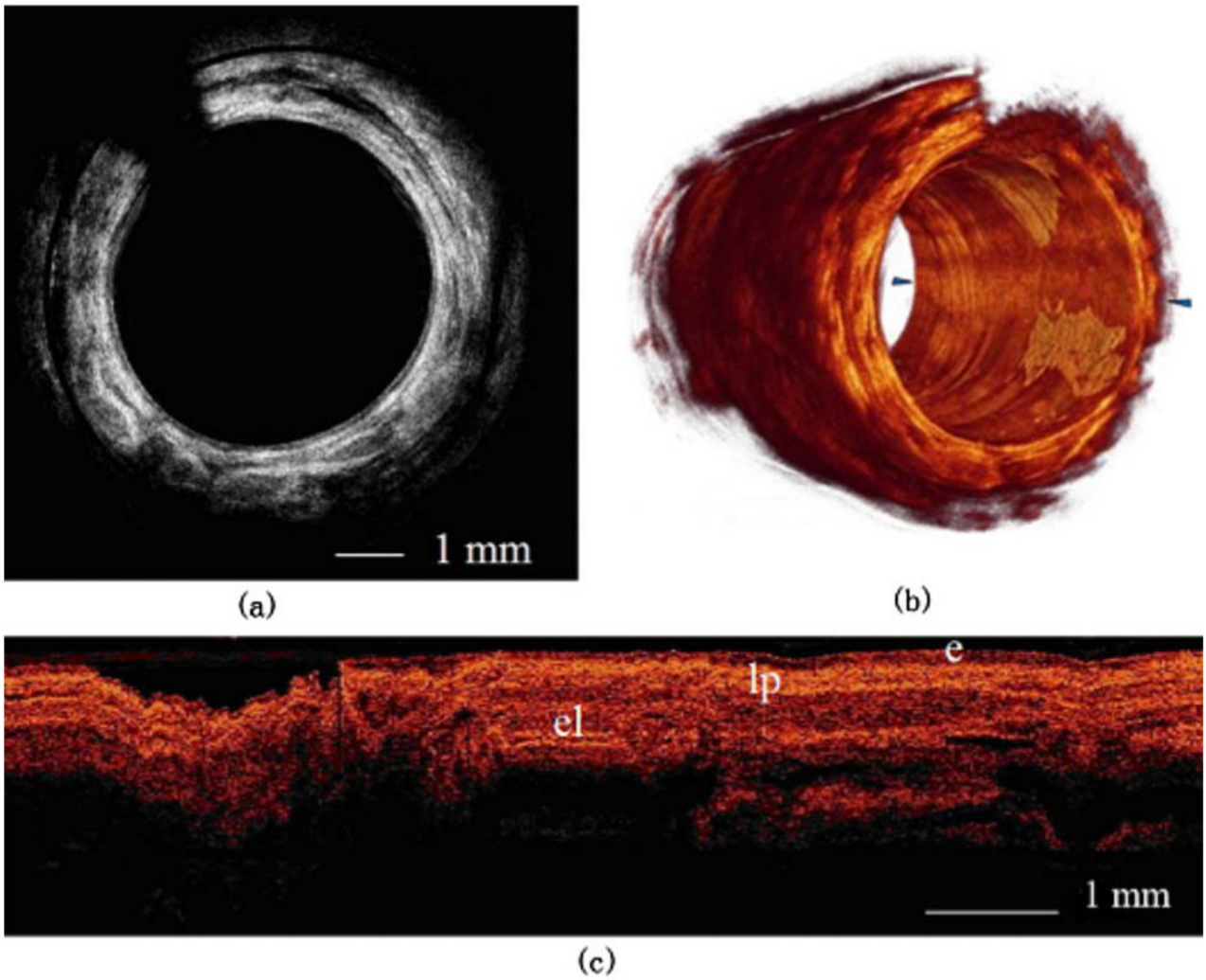

Fig. 3.
(a) One slice of the human lower left lobe bronchus. The dent is an artifact of the MEMS motor wire. (b) 3-D reconstruction of 400 slices from part (a). The longitudinal length is 8.2 mm (e=epithelium; lp=lamina propria; el=elastic lamina). (c) Longitudinal image slice rebuilt between the two arrows in part (b).

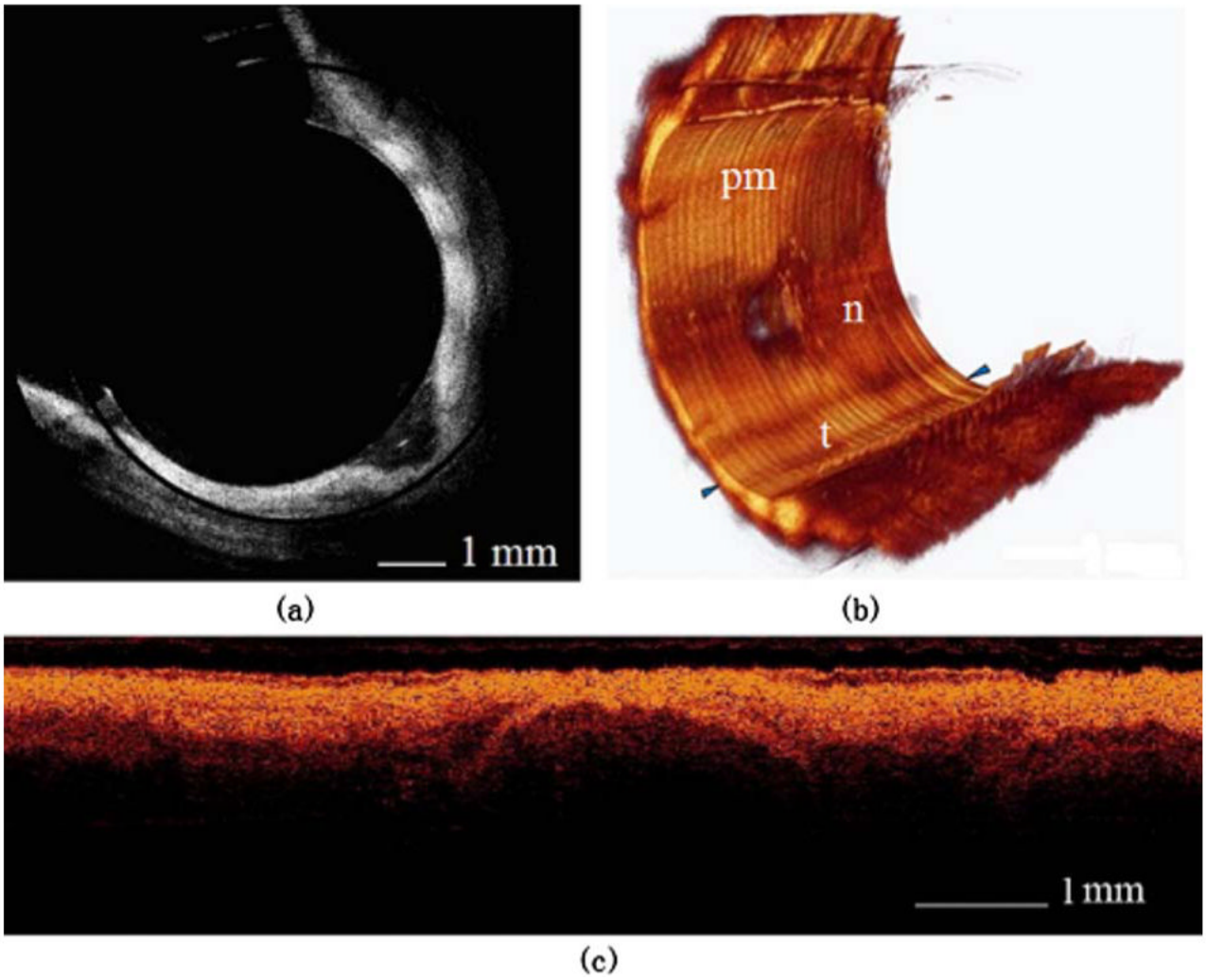

Fig. 4.

(a) One slice of the human distal trachea. Only part of the tissue is inside the imaging range. (b) 3-D reconstruction of 400 slices from part (a). The longitudinal length is 8.2 mm (pm=posterior membrane; n=notch; t=trachea). (c) Longitudinal image slice rebuilt between the two arrows in part (b). The cartilage arc can be seen in the middle.